Water Masses, Mass Transport and Variability of the Canary Current in Autumn

CHRISTINA ANN MOCK

Facultad de Ciencias del Mar, Universidad de Las Palmas de Gran Canaria, Las Palmas, Spain

Abstract

CTD casts from four separate autumn cruises in 1997, 2003, 2006, and 2009 sampled the Canary Basin in order to describe the autumn characteristics of the Canary Current. To calculate geostrophic velocities and transport, a reference level of no motion of y_n = 28.072 kg m^{-3} (approximately 3000 m depth) was chosen to integrate the thermal wind equation, as supported from LADCP data used from the ORCA 2009 campaign. In autumn, the average section shows a Canary Current flowing to the south at a rate of -3.6 Sv (1 Sv = 10^9 kg s^{-1}) in the surface layer (0-700 m) at the latitude of the Canary Islands, from the African coast to 18ºW. This net flow is divided into a northward component of 1.1 Sv in the Lanzarote Passage (LP) and a southward component to the west of Lanzarote Island of -4.7 Sv transporting North Atlantic Central Water (NACW). In the intermediate layers (700 – 1600 m depth), Antarctic Intermediate Water (AAIW) is transported northward in the LP with 0.7 Sv. West of Lanzarote Island, the intermediate layer transport is nearly negligible although there are high energetic eddies with warm, salty Mediterranean Water (MW) presumably flowing toward the south. Deep water layers have negligible transport fluctuations, consisting of North Atlantic Deep Water (NADW) properties. While the autumn tendency is flow to the north at the surface layers in the LP, fluctuations exist from 2.2 to -1.9 Sv. However, in the intermediate layers the transport is rather consistent with variations from 0.1 to 0.7 Sv to the north, as all show AAIW features in each of the stations sampled in the LP. West of Lanzarote Island, all four cruises show a surface Canary Current component to the south ranging from -4.1 to -5.0 Sv, with the exception of 2009 where the transport is -1.5 Sv.

Key words: water masses, mass transport, Canary Current, annual variation

1.   Introduction

The eastern dynamic boundary of the North Atlantic Subtropical Gyre is defined by the Canary Current which is primarily fed by the easterly branch of the Azores Current and flows southwestward through the Canary Islands and along the Northwestern coast of Africa, turning westward into the North Equatorial Current (Hernández-Guerra et al., 2005; Machín et al., 2006). This southward flow transports surface North Atlantic Central Waters (NACW) across the Canary Islands.

At first, studies of the Canary Current were made using historical data from the general North Atlantic area (Stramma, 1984; Stramma and Siedler, 1988; Stramma and Isemer, 1988) due to the lack of direct sampling in the Canary Island Basin. In the late 1990's, the European Union funded CANIGO (Canary Islands Azores Gibraltar Observations) Project collected data north of the Canary Islands (Parrilla et al., 2002). Four cruises were conducted between Madeira and Canary Islands for each season (Knoll et al., 2002). Machín et al. (2006) applied an inverse box model to examine the seasonal characteristics of the Canary Current. Meanwhile, a more consistent interest continued to research the Canary Basin through the CORICA, RAPROCAN and ORCA projects.

The Canary Current became more defined as the southward transport of surface North Atlantic Central Waters (NACW) across the Canary Islands to approximately 700 m depth (Hernández-Guerra et al., 2001, 2005; Machín et al., 2006). The intermediate waters showed evidence of Mediterranean Water (MW) spreading from the Straits of Gibraltar with saltier, warmer cores crossing the Canary Island Basin. Deep waters consisting of North Atlantic Deep Water (NADW) have shown no predominant direction flow. Likewise, special interest was also taken in the channel between the African coast and Lanzarote Island, the Lanzarote Passage (LP). This area is a shallower region with a

maximum depth of 1300 m. Whereas the Canary Current shows a general mean southward transport, significant seasonal transport variations in the LP were noted (Hernández-Guerra et al., 2002, 2003; Machín et al., 2006, 2010; Fraile-Nuez et al., 2010). Current meter moorings were deployed in the late 1990's in the LP (Knoll et al., 2002; Hernández-Guerra et al., 2001, 2002, 2003). Hernández-Guerra et al. (2003) calculated northward transport of NACW in the LP from these moorings at the surface layer in the autumn and recognized the presence of AAIW in the intermediate levels. Fraile-Nuez et al. (2010) and Machín et al. (2010) used nine years of data to further analyze the mass transport variation in the LP.

The intention of this study is to focus on the Canary Current in the autumn season defining its water masses and calculating the mass transport in this region. Section 2 describes the campaigns used to collect the hydrographic data used in this study and the methods used to calculate geostrophic velocities and mass transport and how the reference level of no motion was determined. Potential temperature/salinity diagrams and vertical sections of potential temperature, salinity and neutral density are used in conjunction with geostrophic velocity and accumulated mass transport diagrams to analyze the net mass transport of the Canary Current in autumn in section 3. The interannual variability is presented in section 4 and the final results are discussed in section 5.

2.   Data and Methodology

This study makes use of four separate cruises that took place during the autumn months in the Canary Island Region. This area encompasses the Canary Basin from 24ºW

eastward along the 29.5ºN parallel until North of Gran Canary Island, then southeast through the islands of Lanzarote and Fuerteventura to the African continental coast, referred to as the Lanzarote Passage (Fig. 1). The mean autumn ensemble was calculated from data where two or more cruise Conductivity-Temperature-Depth (CTD) stations coincided. In this study a total of 32 stations were used to calculate the autumn average, eight of these within the LP. Table 1 shows the corresponding dates and number of CTD stations from each cruise considered in our area of study. 32 of the stations were duplicated at least once in order to provide us means to conduct a study generalizing the characteristics of the Canary Current in the autumn season.

CANIGO is chronologically the first campaign in this study which took place in September 1997 and provides us the most stations in the LP, 12 total. Its stations only extend westward to 18ºW. CORICA is the next fall campaign in which data is taken in 2003. This campaign provides us with 7 stations in the LP, and 24 stations west of Lanzarote, even though in this campaign continues further westward. The RAPROCAN campaign in fall of 2006 provides us data from all 28 of its stations, with 5 in the LP. The ORCA cruise of 2009 is the only campaign of this study to occur during November. It only provides us 2 data stations in the LP. Although 18 data stations are available westward of the LP, only 10 correspond with positions from previous cruises and are used for the ensemble data set. From here out, each cruise will be referred to by its corresponding year and the mean data of the four cruises will be referred to as the average or ensemble.

Generally reflected in the four cruises, data stations are closer together in the LP, as this area samples the continental slope. Stations are closely spaced in order to minimize interpolation errors when calculating mass transport due to the bottom triangle formed by steeper slopes.

Each CTD cast collected temperature and salinity data from dual sensors and water samples from a 24-bottle rosette, with 10 liter bottles. Temperature and pressure sensors were calibrated in accordance with WOCE standards at the SeaBird laboratory. Salinity measurements were calibrated onboard by analyzing water samples with a Guildline AUTOSAL 8400B salinometer with accuracy better than 0.002 for single samples (salinity values are noted in the Practical Salinity Scale). Conductivity measurements were calibrated with the application of slope correction.

In all four campaigns, potential temperature, θ, and salinity, S, were obtained from CTD measurements at each station with values gridded to a vertical resolution of 2 dbar. Neutral density, γ_n, was computed according to Jackett and McDougall (1997).

On the ORCA 2009 cruise, the Lowered Acoustic Doppler Current Profiler (LADCP) system employed a two Teledyne/RDI Workhorse (WH) 300 kHz, which were mounted on the rosette and deployed at each CTD cast. Both narrow band units were run in master/slave mode, one upward looking (slave) and one downward looking (master) with a shared battery pack. LADCP data was processed with the Visbeck software, developed at Colombia University (Fischer and Visbeck, 1993). A GPS reference is applied to calculate the absolute velocity. In order to compare the LADCP velocities with geostrophic velocities, the barotropic tidal component was subtracted from each LADCP profile. Using the OSU (Oregon State University) TOPEX/POSEIDON global tidal model (TPXO), the tidal component was predicted for 2009, using the bottom track time, halfway through CTD cast, as the time for the tidal prediction. (Comas-Rodríguez et al., 2010).

Geostrophic velocities are calculated using the thermal wind equation. In order to correctly integrate this equation, a reference level with a known velocity is necessary. Usually the reference level is chosen at the level of no motion, or zero velocity that is

unknown. In order to determine which reference levels of no motion could be considered more accurate for our study, we use the LADCP data from 2009 cruise, the only one with these measurements. Geostrophic velocities are computed with different levels and compared with the LADCP velocities following a similar procedure as described in Comas-Rodríguez et al. (2010).

Initially, a neutral density of 28.072 kg m^{-3} for the reference level of no motion was chosen as per Hernández-Guerra et al. (2005). This level is located at approximately 3000 m depth. This reference level also is supported in the study of the North Atlantic carried out by Ganachaud (2003). However, when the sea floor is shallower than the reference isoneutral, the sea bottom becomes the reference level. Likewise, calculations were made with reference level values of γ_n = 27.38 kg m^{-3} (approximately 700m) for shallow-water stations and γ_n = 27.922 kg m^{-3} (approximately 1600m) for deep-ocean stations in accordance with Machín et al. (2006).

Figure 2 shows the results considering both reference layers. Figure 2a shows the θ/S diagram for the 2009 cruise where Antarctic Intermediate Water (AAIW) is clearly seen in the LP (Hernández-Guerra et al., 2001, 2003, 2005; Machín et al., 2006, 2010; Fraile-Nuez et al., 2010). This AAIW is transported by a north flow due to the stretching of intermediate water strata as stated by Machín et al. (2010). LADCP transport in Figure 2c shows this northward flow at intermediate layers in the LP as well as the geostrophic transport referenced to 28.072 Υ_n. As previously mentioned, in the case of the LP, where the maximum γ_n < 27.82, the reference level is the sea bottom. In contrast, the geostrophic transport referenced to 27.38 Υ_n shows a southward transport.

It is well known that the surface transport in the LP in autumn is to the north (Machín et al., 2006, 2010; Fraile-Nuez et al., 2010). Figure 2b shows that the LADCP transport represents this northward flow in the LP. As in intermediate layers, the

northward geostrophic transport in the surface layer is obtained using a reference layer at 28.072 Υ_n and not 27.38 Υ_n. Westward of the LP, geostrophic transport from both reference layers shows a similar behavior and roughly agree with the LADCP transport. Although the overall Canary Current transport visually looks similar for both sets of reference layer values, the 28.072 Υ_n is chosen because it correctly reflects the northern transport in the LP. Overall, the greatest correspondence is seen with the 28.072 Υ_n reference layer.

3.   Autumn Average Transport

As mentioned before, the data from stations where 2 or more CTD casts from different cruises coincided were combined to create the average autumn ensemble, consisting of 32 stations. Fig. 3 displays the θ/S diagram which demonstrates four notable vertical regions; two with wide variability (surface and intermediate waters) and two with close clustering (NACW and NADW). Superimposed are σ_θ isolines which help define different water layers (surface, intermediate and deep; σ_θ = 26.5, 27.3, and 27.9, respectively). The shallowest layer above the seasonal thermocline (approximately 70 m) is represented by a scattering of θ/S values due to seasonal heating, evaporation and low-salinity water advected by upwelling filaments generated off the northwest African coast during autumn (Van Camp et al., 1991; Hernández-Guerra et al., 1993; Nykjaer and Van Camp, 1994; Barton et al., 1998; Pacheco and Hernández-Guerra, 1999). NACW is seen from the seasonal thermocline to approximately 700 m depth, which corresponds to approximately σ_θ = 27.30 (Harvey 1982). The intermediate stratum ($27.38 < \sigma_\theta < 27.922$, roughly 700 -1600 m depth) contains two different water masses: a relatively fresh (S < 35.4) AAIW and a warmer and saltier (S > 35.5) MW. All 8 stations in the LP contain

AAIW properties in the intermediate water levels as seen in the vertical sections of potential temperature and salinity reflected by the salinity minimum and cooler temperatures (Figures 4 and 5). Likewise, MW is defined by salinity maximum and warmer temperatures, found at stations 18 and 24. A mixture between AAIW and MW is observed in the rest of the sections. A thick deep branch from approximately 1600 m depth to the ocean bottom is occupied by NADW.

In Fig. 4, temperatures range from less than 2°C in deep waters to greater than 23°C at the surface. Surface temperatures are slightly cooler along the African coast and gradually get warmer further into the open ocean. As the surface temperature increases further away from the African coast, similarly there is an increase in salinity as seen in Fig. 5. Average salinity values for autumn along this transect are slightly higher than 37 at the surface and lower than 34.89 in deep waters. The cooler and less saline water in the surface layer close to the African coast is due to the advection of upwelled waters from the African coast to offshore as already mentioned.

In general, salinity decreases with depth, except in intermediate waters near 800 – 1300 m depth where a subsurface salinity maximum is present. This confirms the presence of the aforementioned MW in the θ/S diagram corresponding to salinity maximums at stations 18 and 24 (approximately 17° and 19.3°W) and warm temperature dips. The presence of AAIW in the θ/S diagram is clearly supported by the pronounced salinity minimum pocket of salinity < 35.3 with corresponding cooler temperatures (θ < 9°C) in the LP.

The average neutral density (y_n), in Fig. 6, is calculated from the autumn average values for potential temperature and salinity at each station with values of kg m^{-3}. These isoneutral contours reflect the natural separation of the water column, dividing the ocean into various layers to distinguish different water masses. As sited in Ganachaud (2003),

we recognize 14 layers in the North Atlantic Ocean as noted in Table 2. The upper four layers reflect surface and thermocline waters. The following three layers ($27.38 < y_n^' <$ 27.922 kg m^{-3}) represent intermediate waters, whereas the bottom layers depict deep waters. The first 4 layers, $y_n^' < 27.38$ kg m^{-3}, correctly represent the general characteristics for surface and thermocline waters. At depths less than 750 m, the isoneutrals show upward slope as they approach the African coast. Intermediate waters show sloping in the isoneutrals which correspond to the various appearances of MW and AAIW. The downward sloping in the LP coincides with the influx on AAIW and northward flow. Deep water isopycnals and isoneutrals display a nearly horizontal line with very little sloping depicting nearly no deep water shear flow which corresponds to the chosen reference level at approximately 3000 m depth.

In order to study the transport for the autumn ensemble, geostrophic velocities and mass transport were calculated using thermal wind equation and applying the previously determined reference level of no motion, 28.072 Υ_n. Fig. 7 shows the cross section of the studied transect and its corresponding geostrophic velocities with positive values reflecting a northward flow and thick zero-velocity isolines separating the north/southward currents. This figure is consistent with the northward flow of AAIW in the LP previously shown with a core maximum of 8 cm s^{-1}. West of Lanzarote Island, north of the Canary Island chain, a series of alternating areas of northward and southerly flow is noticed that represents the high eddy field found in this area (Mason et al., 2011). However, the overall flow is mostly dominated and more intense in the southerly flow, specifically between stations 18 and 20 (9 cm s^{-1}) and 22 to 26 (13 cm s^{-1}). These main cores of southerly flow are located in the upper 600 m. This corresponds to NACW flowing to the south. The strongest surface eddies are clearly seen where the zero-velocity isolines divide very strong velocity changes at 15.9º (-8 to 7), 17º (7 to -9), 18º (-

9 to 13) and 18.5°W (13 to -13 cm s^{-1}). Various northward flow cores (average maximum values of 3 cm s^{-1}) are located along the transect in intermediate waters at approximately 15°, 16.5°, 18.3°, and 21.5°W at 1000 m depth. These alternating positive and negative velocities also translate into cyclonic and anticyclonic eddies observed along the transect.

The accumulated mass transport for autumn's average along this section is shown in Fig. 8. The water column is grouped into three different layers corresponding to the surface (y_n < 27.38 kg m^{-3}), intermediate (27.38 < y_n < 27.922 kg m^{-3}), and deep (y_n > 27.922 kg m^{-3}) waters. Ekman transport is applied to the top surface layer by collecting ocean surface wind data from scatterometer QuickScat for the corresponding month and year of each campaign. Mean calculations were obtained from the average of the resultant four Ekman transport estimates. The calculated Ekman transport for the autumn average is 0.3 Sv (1 Sv = 10^6 m^3 s^{-1} ~ 10^9 kg s^{-1}). As in the geostrophic velocity figure, positive values reflect a northern flow.

In the LP a northern transport is clearly present in surface (1.1 Sv) and intermediate (0.7 Sv) waters in concordance with previous discussions. In the surface waters a net flow to the south is experienced west of Lanzarote Island, characterizing the Canary Current. From our study, we define the Canary Current as the stream of water that crosses the Canary Islands, focusing on the area where all 4 stations from the different campaigns coincide, at approximately 18°W. We identify the surface Canary Current with a net value of approximately -3.6 Sv to the south, divided into a northward component of 1.1 Sv in the LP and a southward component of -4.7 Sv transporting NACW southward. Whereas at the intermediate layers, the Canary Current has a net transport of 0 Sv despite various eddies and influx of MW. After the Canary Current, we observe an eddy and, continuing further westward more eddies with a general transport trend to the south. Although the transect is filled with high energetic eddies, the overall

transport to 23.5ºW is approximately -7.4 Sv for the surface layer and -0.3 Sv for the intermediate layer. The eddies seen in the geostrophic velocity section (Fig. 7) are clearly reflected by steep peaks in the mass transport section. The largely defined eddy structure at approximately 17ºW is reflected by strong temperature and salinity maximum patches concentrated at 1000 m depth which coincides with MW.

4.   Interannual Variability

Each campaign was individually analyzed in order to study the interannual variability. Fig. 9 shows the location of stations sampled during each cruise; every black dot represents a CTD cast with the triangles/stars representing the presence of MW/AAIW, respectively. Years 1997 and 2009 are difficult to accurately compare due to the fact that 1997 provides us eight stations in the LP and samples to 18ºW, whereas 2009 has only two casts in the LP and continues to 24.5ºW.

Immediately noticeable in all four campaigns is the presence of AAIW at every one of the LP stations. This is concurrent with the individual θ/S diagrams for each cruise in Fig. 10. AAIW is only found in the LP with the exception of 2006 where patches of AAIW were found to the far west of the Canary Islands and are also reflected in the autumn average mean with low salinity cores at 22º and 24ºW at 1000 m depth in Fig. 4.

Each cruise possesses at least one occurrence of MW between Lanzarote Island and 20ºW shown on the individual θ/S diagrams. MW in 2003 and 2006 have the highest salinity and in both cases are located at two adjacent stations along the transect. The MW in 2003 is quite distinct from the intermediate waters and shows very pronounced

properties. Whereas the intermediate waters in 1997, 2006 and 2009 have more mixing with a tighter clustering of temperature and salinity values.

The accumulated mass transport comparison for each campaign at each layer is shown in Fig. 11. Ekman transport was applied to the top surface layer transport with values of 0.3, 0.6, 0.3, and 0.0 Sv for 1997, 2003, 2006, and 2009, respectively. First looking at the surface layer transport in Fig. 11,top, all cruises show a northern transport in the LP with the exception of 2006. Transport values in the LP are 2.2, 0.9, -1.9 and 0.6 Sv for 1997, 2003, 2006 and 2009, respectively. 2009 has only 2 stations but in the middle of the LP that match the transport in the whole passage (Hernández-Guerra et al., 2003). When defining the Canary Current as the stream crossing the Canary Islands and reaching 18ºW, the first three campaigns coincide with net transport values after Lanzarote Island of -4.2, -5.0, and -4.1 Sv (for 1997, 2003, and 2006, respectively). After Lanzarote Island, 2009 shows a net transport of -1.5 Sv, which is considerably lower than then other cruises. It is worth mentioning that although each campaign showed various eddies throughout the transect, curiously, all 4 campaigns have surface eddies that coincide at 15º and 18ºW.

Similarly in intermediate waters (Fig. 11,middle), all campaigns show a northern transport in the LP with the exception of 2006. After Lanzarote Island the general Canary Current shows little transport with varied net flows of 0.1, -1.2, -1.0, and 0.0 Sv at 18ºW for 1997, 2003, 2006, and 2009, respectively. The three campaigns that continue past 18ºW all show a larger eddies and very little overall transport further west of the Canary Island chain. In deep waters (Fig. 11,bottom), all four campaigns show zero transport in the LP due to the fact that the surface bottom is shallower than $y_n = 27.922$ kg m^{-3}. Very little transport is experienced in the deep layers throughout the studied area due to the chosen reference level.

5.   Discussion

In autumn, the averaged Canary Current flows southward at a rate of -3.6 Sv at the latitude of the Canary Islands, from the African coast to 18ºW. This net flow is divided into a northward component of 1.1 Sv in the LP and a southward component of -4.7 Sv transporting NACW southward. In the intermediate layers, AAIW is transported northward in the LP with 0.7 Sv and very small transport west of Lanzarote Island. Deep water layers have negligible transport fluctuations, containing NADW properties. Throughout the transect, various eddies meander in the Canary Current.

The data field for CORICA 2003 was previously analyzed in Hernández-Guerra et al. (2005) in which the inverse model calculations were applied to the entire hydrographic box, whereas this study just looks at the northern transect of the sampled box. From this study we used the same reference level of no velocity, 28.072 Υ_n. His findings showed a southward Canary Current of -4.7 +/- 0.8 Sv at the latitude of the Canary Islands, from the African coast to 19ºW, divided into a northward net flow of 1.1 +/- 0.5 Sv in the LP and southward component of -5.8 +/- 0.6 Sv. Our study shows a -4.1 Sv Canary Current with a northward net flow of 0.9 Sv and southward component of -5.0 Sv, which these slight differences can be attributed to the fact that the 2006 study extends the Canary Current to 19ºW, where this study ends at 18ºW in order to coincide with the autumn average. We also coincide in the presence of an anticyclonic meddy in the intermediate layers and a net southward flow of -1.2 Sv, similar to the value obtained by Hernández-Guerra et al. (2005).

In comparison with the other campaigns, the 2009 campaign shows weaker transport values with a net transport for the Canary Current of -0.9 Sv to south, with a northward component in the LP of 0.6 Sv and the weakest southward branch in our study of -1.5 Sv. This weaker current is perhaps to be due to the fact that this is the only study that took place in November, two months later than the other cruises.

This study uses data from various campaigns carried out in autumn in which we were fortunate to have 32 of the CTD stations coincide in order to gather data and compile an autumn average ensemble. However, it is still difficult to accurately compare the separate campaigns due to the diverse conditions that each researcher applies, which is our case when choosing of the reference level of no motion. However, even though the reference levels are different, the general results are similar.

References

Barton, E., J. Arístegui, P. Tett, M. Cantón, J. García-Braun, S. Hernández-León, L. Nykjaer, C. Almeida, J. Almunia, S. Ballesteros, G. Basterretxea, J. Escánez, L. García-Weill, A. Hernández-Guerra, F. López-Laatzen, R. Molina, M. F. Montero, E. Navarro-Pérez, J. M. Rodríguez, K. van Lenning, H. Vélez, and K. Wild, 1998: The transition zone of the Canary Current upwelling region. *Prog. Oceanogr.*, **41**, 455–504.

Comas-Rodríguez, I., A. Hernández-Guerra and E. L. McDonagh, 2010: Referencing geostrophic velocities using ADCP data at 24.5ºN (North Atlantic). *Scien. Mar*, **74**, 331-338.

Fischer, J. and M. Visbeck, 1993: Deep velocity profiling with self-contained ADCPs. *J. Atmos. Ocean. Tech.*, **10**, 764-773.

Fraile-Nuez, E., Machín, F., Vélez-Belchí, P., López-Laatzen, F., Borges, R., Benítez-Barrios, V., and A. Hernández-Guerra, 2010: Nine years of mass transport data in the Eastern boundary of the North Atlantic Subtropical Gyre. *J. Geophys. Res.*, **115**, C09009, doi:10.1029/2010JC006161.

Ganachaud, A., 2003: Error budget of inverse box models: The North Atlantic. *J. Atmos. Ocean. Tech.*, **20**, 1641–1655.

Harvey, J., 1982: Ɵ-S relationships and water masses in the eastern North Atlantic. *Deep Sea Res.*, **29**, 1021– 1033.

Hernández-Guerra, A., J. Arístegui, M. Cantón, and L. Nykjaer, 1993: Phytoplankton pigment patterns in the Canary Islands area as determined by using CZCS data. *Int. J. Remote Sens.*, **14**, 1431–1437.

Hernández-Guerra, A., F. López-Laatzen, F. Machín, D. de Armas, and J. L. Pelegrí, 2001: Water masses, circulation and transport in the Eastern Boundary Current of the North Atlantic Subtropical Gyre. *Scien. Mar., 65* (Suppl. 1), 177-186.

Hernández-Guerra, A., F. Machín, A. Antoranz, J. Cisneros-Aguirre, C. Gordo, A. Marrero-Díaz, A. Martínez, A. W. Ratsimandresy, A. Rodríguez-Santana, P. Sangra, F. López-Laatzen, G. Parrilla, and J. L. Pelegrí, 2002: Temporal variability of mass transport in the Canary Current. *Deep-Sea Res. I*, **49**, 3415-3426.

Hernández-Guerra, A., E. Fraile-Nuez, R. Borges, F. López-Laatzen, P. Vélez-Belchí, G. Parrilla, and T. J. MuÄller, 2003: Transport variability in the Lanzarote passage (eastern boundary current of the North Atlantic Subtropical Gyre). *Deep-Sea Res. I*, **50**, 189-200.

Hernández-Guerra, A., E. Fraile-Nuez, F. López-Laatzen, A. Martínez, G. Parrilla, and P. Vélez-Belchí, 2005: Canary Current and North Equatorial Current from an inverse box model. *J. Geophys. Res.,* **110**, C12019, doi:10.1029/2005JC003032.

Jackett, D. and T. J. McDougall, 1997: A neutral density variable for the world's ocean. *J. Phys. Oceanogr.,* **27**, 237-263.

Knoll, M., A. Hernández-Guerra, B. Lenz, F. López-Laatzen, F. Machín, T. Müller, and G. Siedler, 2002: The Eastern Boundary Current system between the Canary Islands and the African Coast. *Deep Sea Res. Part II*, **49**, 3427–3440.

Machín, F., A. Hernández-Guerra, and J. L. Pelegrí, 2006: Mass fluxes in the Canary Basin. *Prog. Oceanog*., **70**, 416-447.

Machín, F., J. L. Pelegrí, E. Fraile-Nuez, P. Vélez-Belchí, F. López-Laatzen, and A. Hernández-Guerra, 2010: Seasonal flow reversals of Intermediate Waters in the Canary Current system east of the Canary Island. *J. Phys. Oceanogr*., **40**, 1902-1909.

Mason, E., F. Colas, J. Molemaker, A. F. Shchepetkin, C. Troupin, J. C. McWilliams, and P. Sangrà, 2011: Seasonal variability of the Canary Current: A numerical study. *J. Geophys. Res.,* doi:10.1029/2010JC006665, in press.

Pacheco, M., and A. Hernández-Guerra, 1999: Seasonal variability of recurrent phytoplankton pigment patterns in the Canary Islands area. *Int. J. Remote Sens*., **7**, 1405–1418.

Parrilla, G., S. Neuer, P.Y. Le Traon, and E. Fernández-Suárez, 2002: Topical studies in oceanography: Canary Islands Azores Gibraltar Observations (CANIGO). Volume 1: Studies in the northern Canary Islands basin. *Deep-Sea Res. II*, **49**, 3409–3413.

Stramma, L., 1984: Geostrophic transport in the warm water sphere of the eastern subtropical North Atlantic. *J. Mar. Res.*, **42**, 537–558.

Stramma, L., and H. Isemer, 1988: Seasonal variability of meridional temperature fluxes in the eastern North Atlantic Ocean. *J. Mar. Res.,* **46**, 281–299.

Stramma, L., and G. Siedler, 1988: Seasonal changes in the North Atlantic Subtropical Gyre. *J. Geophys. Res.,* **93**, 8111–8118.

Van Camp, L., L. Nykjaer, E. Mittelstaedt, and P. Schlittenhardt, 1991: Upwelling and boundary circulation off northwest Africa as depicted by infrared and visible satellite observations. *Prog. Oceanogr*., **26**, 357– 402.

List of Tables

Cruise	Dates	Number of Stations	
		Total	**LP**
CANIGO Poseidon 233	7-18 September 1997	24	12
CORICA	7-29 September 2003	36	7
RAPROCAN 0906	6-16 September 2003	28	5
ORCA	3–8 November 2009	21	2
Ensemble		**32**	**8**

Table 1. Cruise, dates and number of stations used in this study. Ensemble refers to the stations used to calculate the average mean, where 2 or more stations from different campaigns coincide. LP stands for the Lanzarote Passage.

Layer	Lower Interface γ_n kg m^{-3}	Water Mass
1	26.44	surface water
2	26.85	NACW
3	27.162	NACW
4	27.38	NACW
5	27.62	MW/AAIW
6	27.82	MW/AAIW
7	27.922	MW/AAIW
8	27.975	UNADW
9	28.008	MNADW
10	28.044	MNADW
11	28.072	MNADW
12	28.0986	LNADW
13	28.11	LNADW
14	bottom	diluted AABW

Table 2. Layer definitions and approximate equivalences with water masses.

List of Figures

8   Autumn average accumulated mass transport stream functions for different groups of layers corresponding to the surface (layers 1-4, $y_n < 27.38$), intermediate (layers 5-7, $27.38 < y_n < 27.922$), and deep (layers 8-14, $y_n > 27.922$) waters. The integration begins at the coast of Africa. Positive/negative accumulated mass transport reflects northward/southward flow, respectively. The gap in the stream function is at Lanzarote Island. Ekman transport has been applied to the surface layer.

9   CTD stations map for each of the 4 campaigns used in this study. Triangles represent presence of MW, stars represent presence of AAIW. Bathymetry comes from the Sandwell-Smith (1997) database.

10   θ/S diagram for each of the four cruises. Superimposed isolines, σ_θ, as in Fig. 2a.

11   Overall integrated mass transport stream functions for each of the cruises at (top) surface (layers 1-4, $y_n < 27.38$), (middle) intermediate (layers 5-7, $27.38 < y_n < 27.922$), and (bottom) deep (layers 8-14, $y_n > 27.922$) waters. The integrations begin at the coast of Africa. Positive/negative accumulate mass transport reflects northward/southward flow, respectively. The gap in the stream function is at Lanzarote Island. Ekman transport has been applied to the most surface layer.
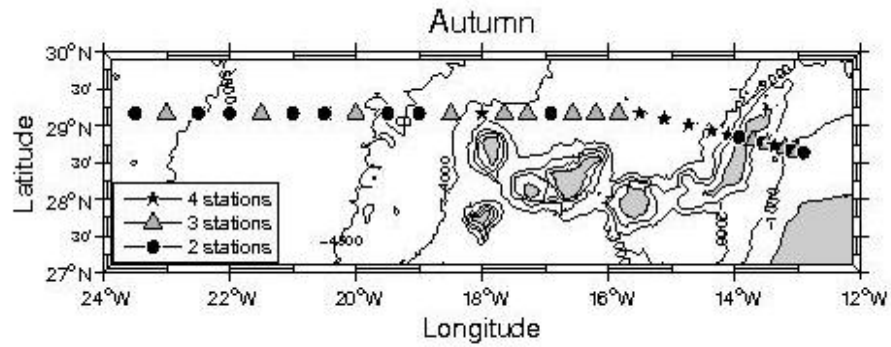
Fig. 1. Area of study, Canary Island Basin. Symbols mark where two (star), three (triangle) or four (circle) CTD stations from different cruises coincide in order to calculate the Autumn Average. For reference, isobaths are shown in meters (Smith and Sandwell, 1997).
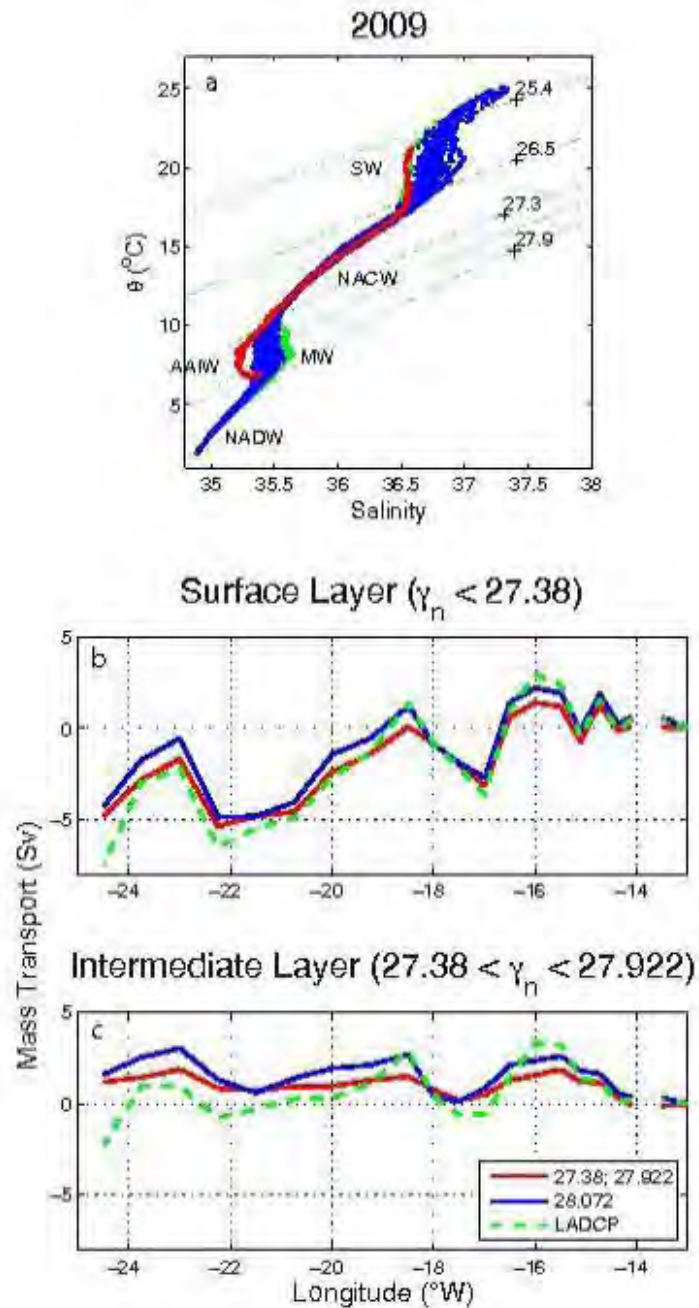
Fig. 2. Data from ORCA 2009 cruise. (a) Potential temperature (θ^oC) / Salinity diagram. Superimposed are σ_θ isolines which help define different water layers (surface, intermediate and deep; $\sigma_\theta = 26.5$, 27.3, and 27.9, respectively). Accumulated mass transport stream functions for (b) surface layer and (c) intermediate waters. Red line indicates reference level of no motion $\gamma_n = 27.38$ kg m^{-3} (~700m) for shallow-water stations and $\gamma_n = 27.922$ kg m^{-3} (~ 1600m) for deep-ocean stations. Blue line represents reference level $\gamma_n = 28.072$ kg m^{-3}, or sea bottom where floor is shallower than isoneutral. Dashed green line represents transport using LADCP data. Positive/negative values reflect northward/southward transport. Ekman transport has been applied to the most surface layer.
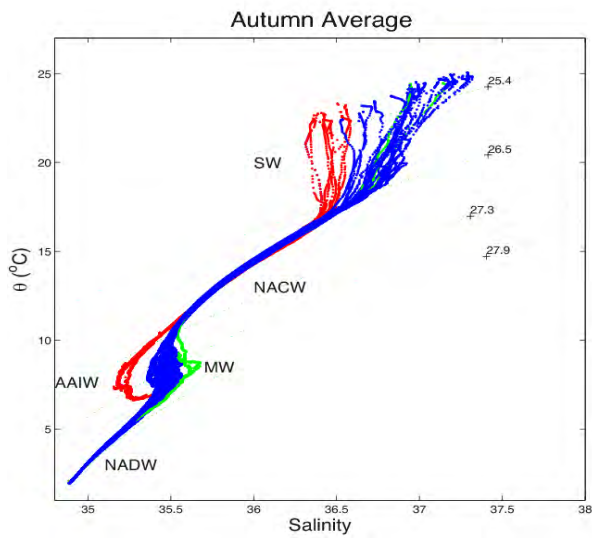
Fig. 3. θ/S diagram using all the data from the four cruises to build an average autumn ensemble. Superimposed isolines, σ_θ, as in Fig. 2a.
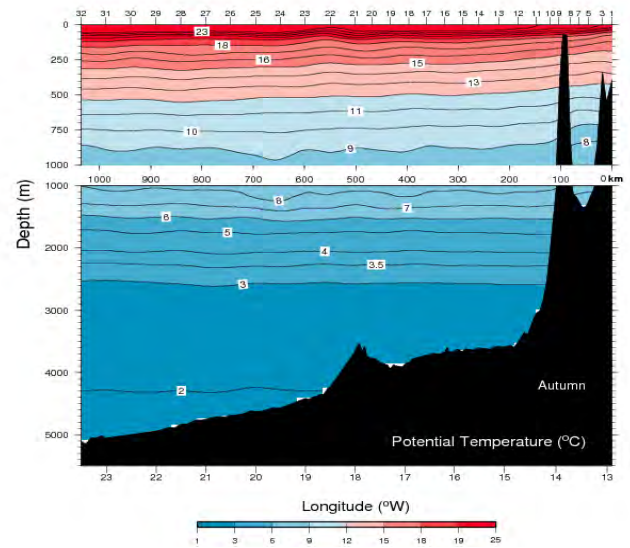
Fig. 4. Autumn average potential temperature vertical section. Bathymetry comes from the Sandwell-Smith (1997) database. Note that the vertical scale changes at 1000 m depth. Top axis indicates autumn average station numbers.
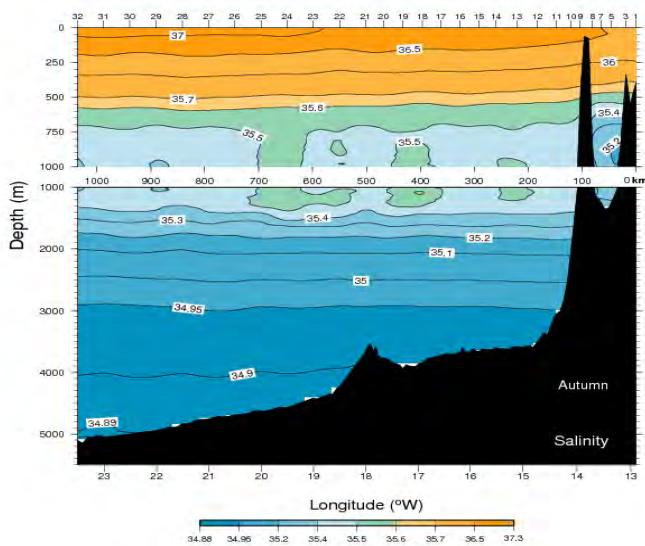
Fig. 5. Same as Fig. 4 but for the autumn average salinity.
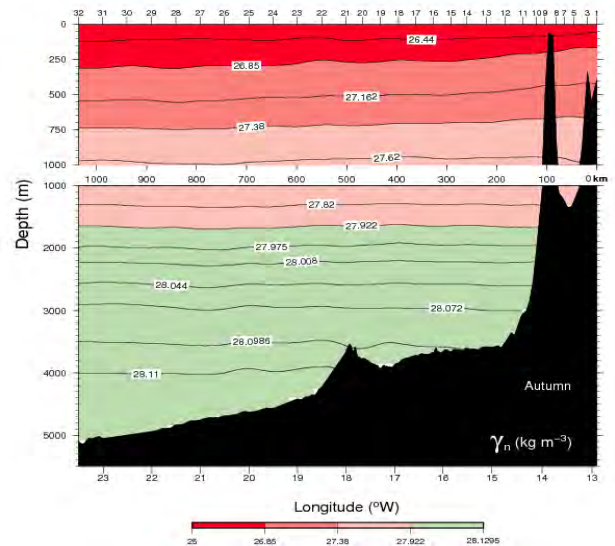
Fig. 6. Same as Fig. 4 but for the autumn average neutral density.
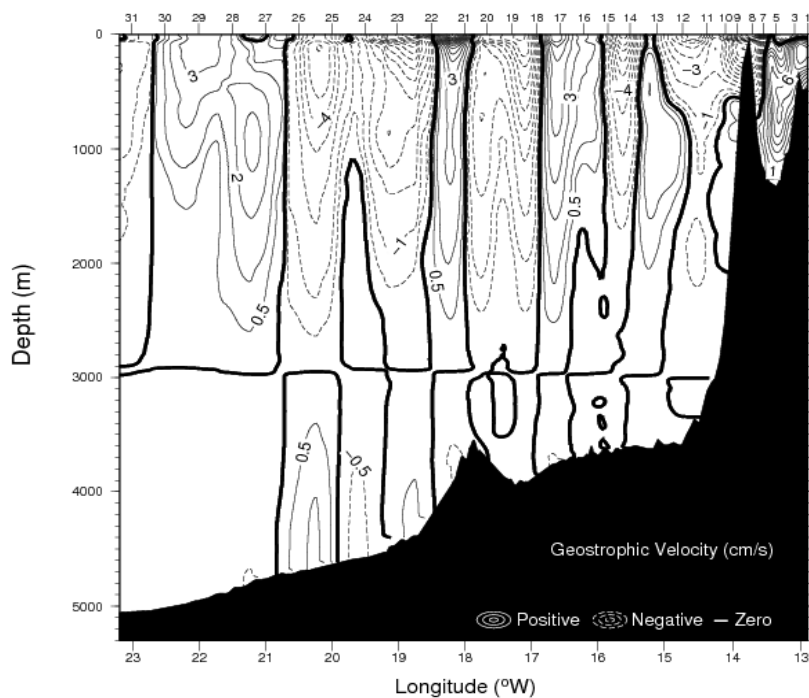
Fig. 7. Vertical section of geostrophic velocity for the autumn average ensemble. Dashed lines correspond to negative (southward) velocities (cm s^{-1}).
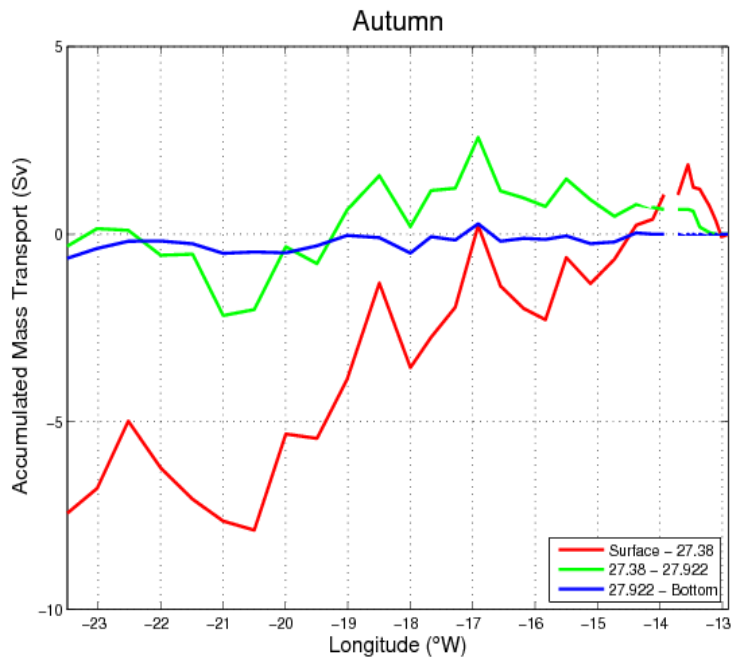
Fig. 8. Autumn average accumulated mass transport stream functions for different groups of layers corresponding to the surface (layers 1-4, $\acute{y}_n < 27.38$), intermediate (layers 5-7, $27.38 < \acute{y}_n < 27.922$), and deep (layers 8-14, $\acute{y}_n > 27.922$) waters. The integration begins at the coast of Africa. Positive/negative accumulated mass transport reflects northward/southward flow, respectively. The gap in the stream function is at Lanzarote Island. Ekman transport has been applied to the surface layer.
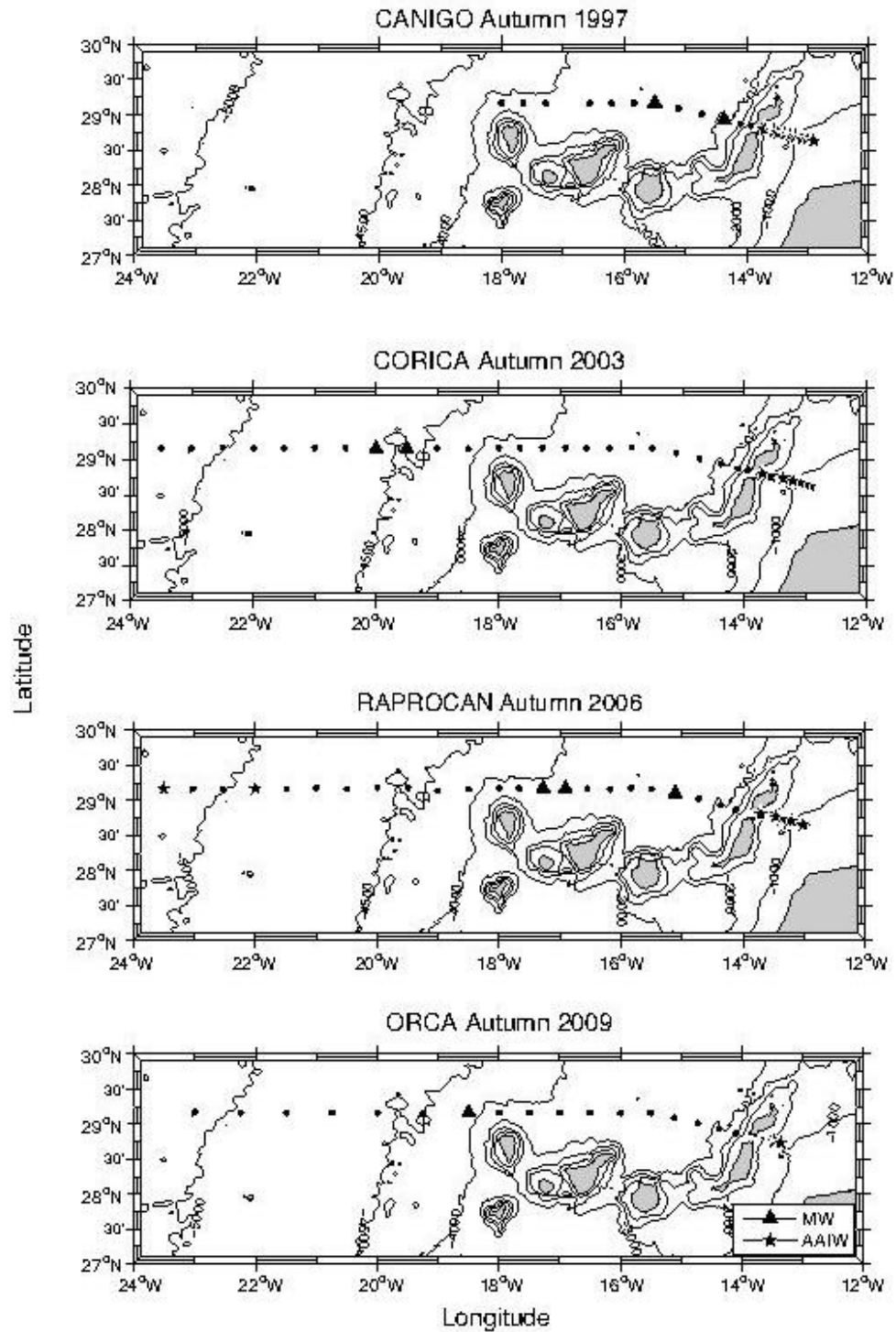
Fig. 9. CTD stations map for each of the 4 campaigns used in this study. Triangles represent presence of MW, stars represent presence of AAIW. Bathymetry comes from the Sandwell-Smith (1997) database.
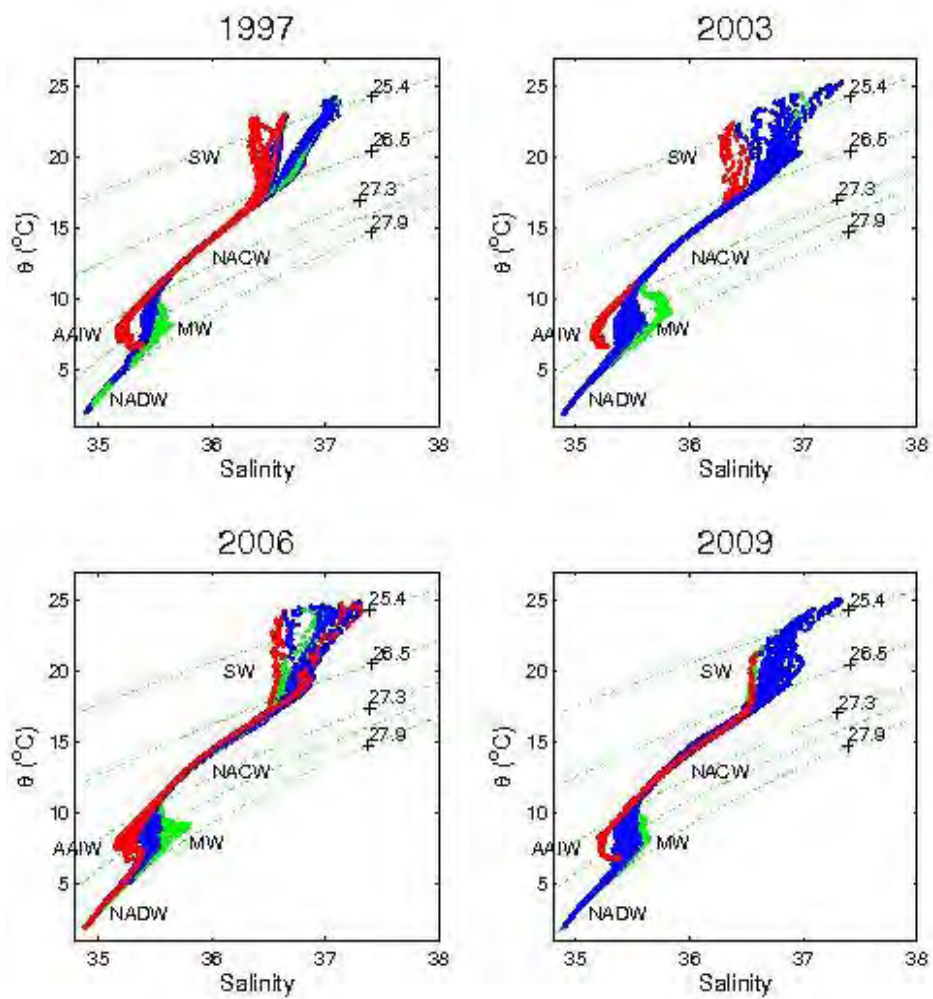
Fig. 10. θ/S diagram for each of the four cruises. Superimposed isolines, σ_θ, as in Fig. 2a.
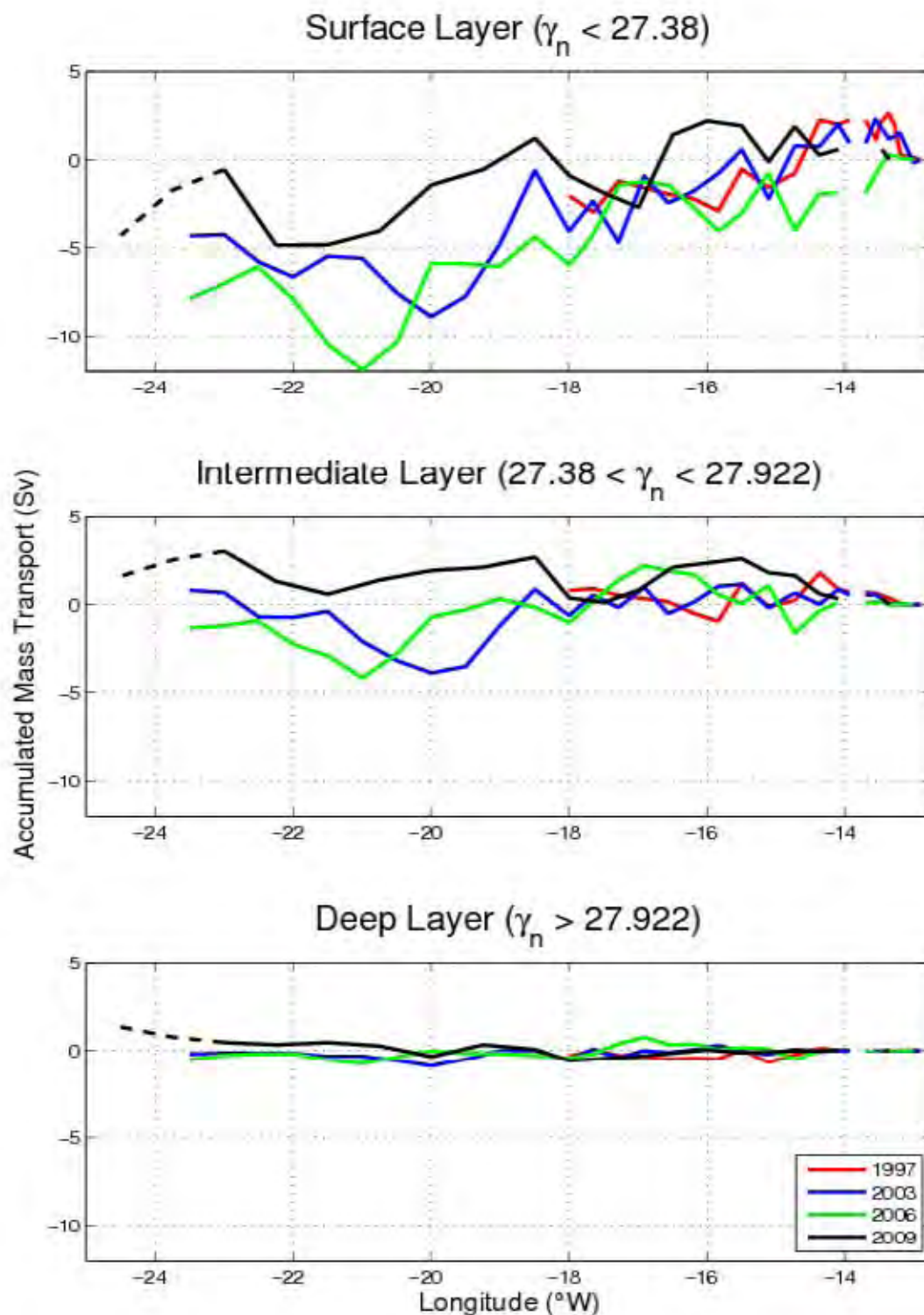
Fig. 11. Overall integrated mass transport stream functions for each of the cruises at (top) surface (layers 1-4, $\gamma_n < 27.38$), (middle) intermediate (layers 5-7, $27.38 < \gamma_n < 27.922$), and (bottom) deep (layers 8-14, $\gamma_n > 27.922$) waters. The integrations begin at the coast of Africa. Positive/negative accumulate mass transport reflects northward/southward flow, respectively. The gap in the stream function is at Lanzarote Island. Ekman transport has been applied to the most surface layer.